

## NRF2 activator A-1396076 ameliorates inflammation in autoimmune disease models by inhibiting antigen dependent T cell activation

Christian Goess<sup>a,\*</sup>, Sonia Terrillon<sup>a</sup>, Martha Mayo<sup>a</sup>, Peter Bousquet<sup>a</sup>, Craig Wallace<sup>a</sup>, Michelle Hart<sup>a</sup>, Suzanne Mathieu<sup>a</sup>, Rachel Twomey<sup>a</sup>, Diana Donnelly-Roberts<sup>b</sup>, Marian Namovic<sup>b</sup>, Paul Jung<sup>b</sup>, Min Hu<sup>b</sup>, Paul Richardson<sup>b</sup>, Tim Esbenshade<sup>b</sup>, Carolyn A. Cuff<sup>a</sup>

<sup>a</sup> AbbVie Bioresearch Center, 100 Research Drive, Worcester, MA, 01605, USA

<sup>b</sup> AbbVie Inc., 1 North Waukegan Rd., North Chicago, IL, 60064, USA

### ARTICLE INFO

#### Keywords:

Antioxidant  
Oxidative stress  
Triterpenoid

### ABSTRACT

Nuclear factor (erythroid-derived 2) like 2 (NRF2) is a nuclear transcription factor activated in response to oxidative stress that induces a gene program that dampens inflammation and can limit cell damage that perpetuates the inflammatory response. We have identified A-1396076, a potent and selective NRF2 activator with demonstrated KEAP1 binding and modulation of cellular NRF2 mediated effects. *In vivo* administration of A-1396076 inhibits inflammation across several rodent models of autoimmunity when administered at or before the time of antigen challenge while also inducing NRF2 modulated gene transcription in the liver of the animals. It was not effective when administered after the time of antigen challenge or in a T cell independent model of arthritis induced by passive transfer of anti-collagen antibodies. A-1396076 inhibited antigen dependent T cell activation as measured by IFN- $\gamma$  production in an *ex vivo* re-stimulation assay and following anti-CD3 challenge of MOG-sensitized mice. A-1396076 reduced costimulatory molecule expression on dendritic cells in the lungs of OVA LPS challenged mice suggesting that the mechanism of T cell inhibition was mediated at least partially by interfering with antigen presentation. These data suggest that NRF2 activation may be an effective strategy to dampen inflammation for treatment of autoimmune disease.

### 1. Introduction

The nuclear factor (erythroid-derived 2) like 2 (NRF2, NFE2L2) drives an anti-oxidant response as well as inhibits inflammatory gene pathways upon release by its cytosolic repressor KEAP1 [1,2]. Under homeostatic conditions KEAP1 sequesters NRF2 in the cytosol, facilitating its poly-ubiquitination and proteosomal degradation [3]. Upon activation by electrophiles and other reactive compounds, KEAP1 releases NRF2 to translocate to the nucleus where it induces the transcription of a wide array of antioxidant, detoxification, and anti-inflammatory genes [4–6].

Induction of the NRF2 pathway through endogenous or exogenous activators leads to the amelioration of inflammation. Mice deficient in NRF2 exhibit an increase in inflammatory response to stimuli which is consistent with the hypothesis that NRF2 activation serves as a brake to the inflammatory response. These mice have been tested in a variety of systems and the data is remarkably consistent. Female NRF2 knockout mice spontaneously develop a lupus-like phenotype characterized by

autoantibody production and immunoglobulin deposition with concomitant nephritis [7]. The NRF2 knockout mice also display more severe and accelerated joint destruction in both the adjuvant induced and KBxN serum transfer models of arthritis [8,9]. Similar exacerbation of inflammation is observed when experimental autoimmune encephalitis (EAE) is induced through sensitization with myelin oligodendrocyte peptide (MOG) resulting in increased inflammation of the optic nerve and more severe sensory motor dysfunction compared to wild type littermates [10].

These knock-out data demonstrate that NRF2 plays a significant role in reducing ongoing inflammation; however, it remains unclear whether pharmacologic activation of the NRF2 pathway would further reduce inflammation. To address this question requires the use of pharmacologic tools that are specific for the activation of the NRF2 pathway and have sufficient drug-like properties to enable the interrogation of the pathway in a whole animal system. Dimethyl fumarate (DMF), currently approved for the treatment of multiple sclerosis under the name Tecfidera,

\* Corresponding author.

E-mail address: [Christian.goess@abbvie.com](mailto:Christian.goess@abbvie.com) (C. Goess).

activates the NRF2 pathway. DMF can activate the NRF2 pathway in multiple cell types including cardiomyocytes, osteoclasts, and keratinocytes [11–13]. Although DMF has demonstrated efficacy in multiple models of inflammation, several lines of evidence suggest that this may be mediated in part through a NRF2 independent mechanism. In a murine dextran sulfate sodium induced colitis model, DMF reduced weight loss, increased colon length, prevented histological damage, and reduced pro-inflammatory cytokine mRNA [14]. DMF reduced disease severity, histological damage, and mortality in a model of graft-versus-host disease [15]. In an EAE model, prophylactic treatment with DMF impacted disease course, reduced histopathological damage in the CNS, and reduced infiltration of macrophages into the spinal cord [16]. NRF2 independent pathways are responsible for mediating efficacy in an EAE model as DMF reduced multiple measures of CNS inflammation in NRF2 knock-out mice [17]. In addition, DMF inhibited NfκB pathway activation in the Ramos human B-lymphocytic cell line and in mouse splenocytes in a NRF2 independent manner [18]. DMF can also inactivate GAPDH to decrease aerobic glycolysis and modulate anti-inflammatory activity [19]. Thus, these data demonstrate that DMF is not an optimal molecule for evaluating the role of NRF2 activation in ameliorating inflammation.

We therefore developed A-1396076, a potent and selective NRF2 activator, through a medicinal chemistry effort to explore the anti-inflammatory efficacy of this class of compounds. A-1396076 is a synthetic triterpenoid molecule that potently binds KEAP1 to drive NRF2-mediated activities. This compound has sufficient drug-like properties to enable *in vivo* pharmacologic interrogation of the role of NRF2 activation on inflammation. In this manuscript we describe the cellular mechanism that may underlie some of the anti-inflammatory effects of NRF2 activators previously reported. For example, other triterpenoid compounds such as bardoxolone methyl suppresses LPS-induced cytokine expression in human neutrophils and peripheral blood mononuclear cells *in vitro* [20]. RTA-408, another triterpenoid, can attenuate the gene expression of several inflammatory mediators in IFN $\gamma$ -activated RAW 264.7 cells [21]. Using the potent and selective molecule A-1396076 we show that NRF2 activation induces a NRF2 driven gene program which correlates with inhibition of inflammation in multiple inflammatory disease models when administered at or before the time of antigen challenge. Mechanistic assays demonstrated that this effect was mediated, at least in part, through inhibition of antigen presentation.

## 2. Methods

### 2.1. KEAP1 binding assay

The competitive TR-FRET based binding assay used His-tagged KEAP1 BTB protein domain, a terbium labeled anti-His antibody, and an Oregon Green labeled probe linked via 2,2'-(ethylenedioxy)bis(ethylamine) to 2-Cyano-3,12-dioxooleana-1,9(11)-dien-28-oic acid (CDDO). 2-Cyano-3,12-dioxooleana-1,9(11)-dien-28-oic acid (CDDO, Syncom) was coupled with benzotriazol-1-yl-oxytripyrrolidinophosphonium hexafluorophosphate to a 10-fold excess of 2,2'-(ethane-1,2-diylbis(oxy))bis(ethan-1-amine) in dimethylformamide and purified to homogeneity by reverse-phase HPLC to give CDDO-PEG2-NH $_2$  which was then coupled to Oregon Green-6-O-succinimidyl ester (ThermoFisher Scientific) to give the desired CDDO-PEG2-OG488 (after RP-HPLC validated pure by LC-MS single peak, ESI-MS  $m/z$  1016.4 [M+H] $^+$ , 1048.3 [M + MeOH + H] $^+$ ; 1014.3 [M - H] $^-$ ).

A fresh assay mixture was prepared with 2.0 nM LanthaScreen Elite Tb-anti-HIS antibody (ThermoFisher Scientific, Waltham MA, USA), 2.5 nM (((Trx-His6-(Thr)-Stag-(EK)-AM-[KEAP1(h) (49–179)] e.coli), 20 nM CDDO-OG488 probe, 5  $\mu$ M dithiothreitol (ThermoFisher Scientific) in a buffer of 47 mM HEPES (pH 8) (ThermoFisher Scientific), 0.9 mM EDTA (ThermoFisher Scientific), 47 mM NaCl (Sigma Aldrich, St. Louis, MO, USA), and 0.0071% Triton X-100 (ThermoFisher Scientific). A 12-point 1:3 dilution of A-1396076 was prepared in White ProxiPlate-384 Plus

plates (PerkinElmer, Waltham, MA, USA). 20  $\mu$ L Assay Mixture was added the 410 nL compound solution already in the plate, yielding a final top compound concentration of 200  $\mu$ M (2.0% DMSO). After the plates were incubated at room temperature for 2 h in darkness, the fluorescence ratio was measured at 520 nm and 495 nm using the TR-FRET enabled EnVision plate reader (PerkinElmer). Dose-response curves were generated using a variable slope curve. The assay was performed with duplicate plates and repeated on multiple days. Testing with His-tagged, full-length KEAP1 (1–624) protein yielded similar results. Concentration-response data were analyzed using GraphPad Prism; the IC $_{50}$  values were derived from a single curve fit to the mean data of N = 4 or more as indicated, in duplicates.

### 2.2. ARE reporter assay

Transient transfection of HEK293-F cells (ThermoFisher Scientific, Waltham MA, USA) were carried out using the Freestyle 293 expression system (ThermoFisher Scientific). Cells were transfected with 1 mg DNA of the ARE-Luc2P plasmid (Promega X697X) per liter of cells, which was mixed with 1.3 ml 293 fectin in OPTI-MEM (5% volume of transfection) for 25 min then added to the cells. Cells were grown in a shaking incubator at 125 rpm, 37  $^{\circ}$ C, and 8% CO $_2$  for 5 h, and then frozen in Freestyle media (ThermoFisher Scientific) with 10% DMSO (Sigma-Aldrich) and 10% fetal bovine serum (FBS: ThermoFisher Scientific) at  $-80^{\circ}$ C. Two days prior to assay, cryopreserved cells were re-suspended in Freestyle 293 media supplemented with 5% FBS at a concentration of 250,000 cells/ml. Suspended cells were immediately plated at 10,000 cells/40  $\mu$ L/well on white half-well tissue culture treated 96 well plates (Corning, Manassas, VA). Cell plates were incubated overnight at 37  $^{\circ}$ C with 5% CO $_2$ . The next day, cells were treated with 10  $\mu$ L of serially diluted test compounds (3  $\mu$ M–0.3 nM serially diluted  $\frac{1}{2}$  log in a 10-point curve) from a 5X stock. Tert-butylhydroquinone (tBHQ:112941, Sigma-Aldrich, St. Louis, MO) at 20  $\mu$ M, was used as the positive control and cell culture media was used for basal control. Cell plates treated with compound were incubated overnight at 37  $^{\circ}$ C. The following morning, plates were removed from the incubator and allowed to equilibrate to RT. One-Glo reagent from Promega was used to quantify luciferase expression following manufacturer's instructions. Plates were read on an Envision plate reader set to 0.5s of luminescence integration time (PerkinElmer, Waltham, MA). Raw data was normalized to 20  $\mu$ M tBHQ with basal levels subtracted out. Concentration-response data were analyzed using GraphPad Prism; the IC $_{50}$  values were derived from a single curve fit to the mean data of N = 4 or more as indicated, in duplicates.

### 2.3. Nitric oxide (NO) suppression assay

RAW 264.7, a mouse macrophage cell line, was obtained from American Type Culture Collection (ATCC; TIB-71, Manassas, VA) and maintained in the log phase of growth in Dulbecco's Modified Eagle's Medium (DMEM), 10% heat inactivated fetal bovine serum (FBS) and 100 units/mL antibiotic-antimycotic (AA). All cell culture supplies were obtained from ThermoFisher Scientific (Waltham, MA, USA). RAW 264.7 cells were plated 1 day in advance of experiment at a concentration of 80,000 cells/well onto Cell-bind 96 well plates in a total volume of 100  $\mu$ L. The next day, cells were pretreated with compounds (3  $\mu$ M–0.3 nM serially diluted  $\frac{1}{2}$  log in a 10-point curve) from a 10X stock, by adding 10  $\mu$ L/well in complete DMEM media containing 10% FBS. The plates were centrifuged for 3 min at 400 $\times$ g at room temperature followed by 2 h incubation at 37  $^{\circ}$ C. The cells were then incubated overnight at 37  $^{\circ}$ C with 10  $\mu$ L of the insult, interferon gamma (IFN $\gamma$ ; R&D Systems), Minneapolis, MN), from a 10X stock for a final concentration of 20 ng/ml. The plates were centrifuged for 3 min at 400 $\times$ g at room temperature followed by  $\sim$ 18-h incubation at 37  $^{\circ}$ C. The following day, 50  $\mu$ L of cell culture supernatant from each well was transferred into a clear bottom 96 well plate for analysis. The Griess Detection Kit from Promega (G2930) was used and the manufacturer's instructions were followed. Within 30

min, absorbance was read to measure the amount of nitrite released. To determine the ability of compounds to suppress the increase in nitric oxide release, the percent maximal intensity of nitrite detected in each well was normalized to that induced by the peak value for 20 ng/ml of IFN $\gamma$  alone and plotted against the compound concentration to calculate IC50 values and to control for plate-to-plate variability. Concentration-response data were analyzed using GraphPad Prism; the IC50 values were derived from a single curve fit to the mean data of N = 4 or more as indicated, in duplicates.

#### 2.4. A-1396076 preparation for *in vivo* use

A-1396076 was prepared and dosed as an amorphous solid dispersion (ASD) containing A-1396076, vitamin E TPGS (BASF, Florham Park, NJ), and copovidone (BASF, Florham Park, NJ) at a ratio of 15/20/65 by weight. Briefly, vitamin E TPGS and copovidone were dissolved in methanol and dichloromethane in a rotating round bottom flask until clear solution obtained. A-1396076 was added to the solution and rotation continued until all components dissolved. Solvent was evaporated at 40C until majority of solvent was gone then allowed to further dry for 90 min prior to being placed into a vacuum oven to dry overnight. For *in vivo* studies, ASD containing A-1396076 was suspended in 0.2% hydroxymethylcellulose (Sigma-Aldrich, St. Louis, MO) and administered at the indicated doses. Indicated doses refer to the amount of A-1396076 dosed rather than total ASD amount. ASD with vitamin E TPGS and copovidone without A-1396076 was used as a vehicle control in all animal studies.

#### 2.5. Animal use and care

Female Lewis rats age 6–8 weeks were purchased from Charles River Labs (Portage, MI). NZB/W F1 mice were purchased from Jackson Laboratories (Bar Harbor, ME). C57/BL6 mice were purchased from Taconic Biosciences (Rensselaer, NY). Male DBA1/J mice were purchased from Jackson Laboratories (Bar Harbor, ME). Female Brown Norway rats (12 weeks old) were purchased from Charles River Labs (Wilmington, MA). Balb/cN mice were purchased from Taconic Biosciences (Rensselaer, NY). SJL/J mice were purchased from Jackson Laboratories (Bar Harbor, ME). All animals were acclimated in the facility for at least seven days prior to use with rats were housed three per cage and mice housed five per cage on a 12 h light dark cycle with food and water provided *ad libitum*. All animal studies were performed in accordance with and under protocols approved by the AbbVie Bioresearch Center Institutional Animal Care and Use Committee (IACUC) in accordance with the Principles of Laboratory Animal Care and all applicable national and local laws.

#### 2.6. Rat adjuvant induced arthritis

Female Lewis rats under light anesthesia were given a single intradermal injection of 200  $\mu$ g Mycobacterium Tuberculosis (Difco Labs, Detroit, MI) in 0.1 ml mineral oil in the right hind paw on day 0. A-1396076 was administered at the indicated doses orally once per day prior to administration of mycobacterium. Contralateral paw volumes were measured using a water displacement plethysmometer, (Ugo Basile North America, Schwenksville, PA) throughout the study approximately every 2–3 days. On day 17 the animals were euthanized by isoflurane asphyxiation, blood was collected by cardiac puncture, and the ankle joints were placed in formalin for a minimum of 48 h. For gene expression evaluation, livers were collected and snap frozen on D17.

#### 2.7. IFN- $\alpha$ accelerated lupus nephritis

Female NZB/W-F1 mice were approximately 14 weeks of age at study start. Mice were randomly assigned to treatment groups (n = 16 mice per group) and were ear-tagged for individual identification. On Day 0, all mice received an IV injection of  $5 \times 10^9$  IFN $\alpha$ -expressing adenovirus particles (Welgen Inc, Worcester, MA) in 100  $\mu$ l PBS. Body weight and

urine protein monitoring were carried out weekly beginning day –8 and day –1 prior to the adenovirus administration. Urine protein levels were measured using Albustix: Reagent Strips for Urinalysis (Seimens Medical Solutions, Malvern, PA). Mice were considered severely proteinuric based on the following criteria: 1) Two consecutive weekly grades of urine protein  $\geq 300$  mg/dL or 2) When reaching grade of urine protein  $\geq 300$  mg/dL prior to death or euthanasia. Moribund animals were euthanized, and the dates recorded. A-1396076 was administered at the indicated doses orally once per day beginning on Day –7. Mycophenolate mofetil (Genentech, San Francisco, CA) was used as a positive control, dosed orally once per day at 100 mg/kg.

#### 2.8. Rat MOG experimental autoimmune encephalomyelitis

Rat myelin oligodendrocyte glycoprotein (MOG) amino acids 1–55 (BlueSky Biotech) was dissolved in PBS at a concentration of 2 mg/ml. Complete Freund's Adjuvant (CFA) was made by adding Mycoplasma tuberculosis, strain H37RA (Difco Labs, Detroit, MI) to IFA at a concentration of 5.5 mg/ml. An emulsion of CFA and MOG was used to immunize rats at the base of the tail (100  $\mu$ g MOG in 100  $\mu$ l). Animals were monitored daily for the onset of clinical signs and scored using the scale: 0 = normal, 1 = limp tail, 2 = abnormal gait, 3 = partial hind limb paralysis, 4 = complete hind limb paralysis, 5 = moribund or dead. Animals that were moribund or lost more than 20% of original body weight were sacrificed for humane reasons. A-1396076 was administered orally once per day (10 mg/kg) beginning either on Day 0 (prophylactic) or Day 7 (late prophylactic/prior to onset of clinical signs). FTY720, a SIP agonist, administered daily (1 mg/kg PO) beginning Day 7 was used as the positive control. Area under the curve was calculated for EAE score over the course of disease and used to calculate percent inhibition. One-way ANOVA was used to determine significance (n = 10 animals/group).

#### 2.9. Rat collagen induced arthritis

Lewis rats were immunized with 600  $\mu$ g bovine type II collagen (Elastin Company, Owensville, MO) in incomplete Freund's adjuvant (IFA) (Difco labs, Labs, Detroit, MI) intradermally on day 0 on the base of tail, left flank, and right flank and boosted with collagen in IFA near the same locations on day 6. Paw volume was measured using a micro-controlled volume meter plethysmograph (Ugo Basile, Italy) with left and right paw volumes averaged for analysis. Paw volume baseline was assessed on day 8 (baseline), 11, 13, 15, and 18. Rats were dosed orally BID at 10 mg/kg beginning on day 5 (late prophylactic) or day 11 (therapeutic) with A-1396076. Prednisolone was used as a positive control and was dosed orally QD starting on day 11. On day 18, plasma was collected to measure anti-collagen antibodies. For gene expression evaluation, livers were collected and snap frozen on D18.

#### 2.10. Mouse GPI induced arthritis

Male DBA1/J mice were immunized intradermally (i.d.) at the base of the tail with 100  $\mu$ l of 1:1 (v/v) emulsion containing 300  $\mu$ g of Glucose-6-phosphate isomerase (AbbVie, Worcester, MA) and 200  $\mu$ g of heat-inactivated *Mycobacterium tuberculosis* H37Ra (Complete Freund's Adjuvant, Difco Labs, Detroit, MI). A-1396076 was dosed orally at 10 mg/kg once per day from day 0–17 or day 7–17. Beginning seven days after immunization, mice were monitored for arthritis. Rear paw size was evaluated using spring calipers (Dyer, Lancaster, PA) on days 7, 10, 13, 15, and 17. Mice began to show signs of paw swelling between day 7 and 10. At the termination of the experiment, 5 livers per group were weighed and samples collected for gene expression analysis.

#### 2.11. Collagen antibody induced arthritis

Arthritis was induced in female Balb/cN by an intravenous (iv) injection of an arthritogenic cocktail of five monoclonal antibodies to type

II collagen (Chondrex, Redmond, WA) on day 0, followed on day 3 by an intraperitoneal (ip) injection of 50  $\mu$ g LPS. Mice were then monitored daily for disease development from day 3 until the conclusion of the experiment. Clinical arthritis in each paw was graded as Mean Arthritic Score (MAS) of 0–3 according to presence of redness and swelling at one or more sites (1), two or more sites (2), or deformity in the paws and stiffness in the joints (ankylosis) (3). A-1396076 was administered orally once per day (3 or 10 mg/kg) beginning on Day 0 (prophylactic). At the termination of the experiment livers were collected from 5 animals per group, weighed, and analyzed for NRF2 dependent gene expression.

### 2.12. MOG/anti-CD3 challenge

An emulsion was prepared with 5 mg/mL MOG (New England Peptide, Gardner, MA) dissolved in PBS and 10 mg/mL heat-inactivated *Mycobacterium tuberculosis* H37Ra (Difco Labs, Detroit, MI) suspended in Incomplete Freund's Adjuvant (Difco Labs, Detroit, MI) at a 1:1 ratio (v/v). Female C57/BL6 mice were immunized with 100  $\mu$ l total volume spread over 3 injection sites SC. Mice also received an ip injection of pertussis toxin (List Biological Labs, Campbell, CA) at 150 ng/mouse in 200  $\mu$ l PBS. 5 days after immunization, mice were iv challenged with anti-CD3 (BD Biosciences, San Jose, CA) prepared in 1% normal mouse serum in PBS at 1  $\mu$ g/mouse. Mice were terminally bled for plasma cytokine levels at 2 h post challenge. Mice were dosed orally with A-1396076 either BID from the day of immunization until the day of challenge or a single dose of treatment given 4 h prior to challenge. An LCK inhibitor [22] was used as a positive control and was dosed at 30 mg/kg orally 1 h prior to anti-CD3 challenge. Study control groups were included which received either the MOG immunization or the anti-CD3 challenge alone.

### 2.13. Mouse ovalbumin lung inflammation

Balb/C mice were sensitized to ovalbumin on day 0 and 7 with an i.p. injection of 8  $\mu$ g ovalbumin (Sigma-Aldrich, St. Louis, MO) in 2 mg Alum Imject (Thermo-Fisher-Scientific, Waltham, MA). On days 14 and 16, animals received intra-nasal challenge of 0.3  $\mu$ g ovalbumin or 0.3  $\mu$ g ovalbumin/100 ng LPS (Sigma-Aldrich, St. Louis, MO). On day 17 the lungs were lavaged 3 times with 0.5 ml PBS/EDTA (Invitrogen, Carlsbad, CA) and the lavage fluid pooled and a cell pellet collected by centrifugation for flow cytometric analysis. Mice were treated orally with indicated doses of A-1396076 BID or with 3 mg/kg dexamethasone beginning on day 13 prior to intranasal challenge. Flow cytometric analysis of bronchoalveolar pellets was performed using anti-CD11c APC, anti-CD80 PCP-Cy5.5, anti-CD86 PE, and anti-MHC Class II FITC antibodies (BD Biosciences, San Jose, CA).

### 2.14. In vitro T cell activation

An emulsion containing 100  $\mu$ g PLP139-151 (New England Peptide, Gardner, MA) in incomplete Freund's adjuvant (Difco Labs, Detroit, MI) supplemented with 200  $\mu$ g *M. tuberculosis* H37Ra (Difco Labs, Detroit, MI) was administered to Balb/C mice subcutaneously over three sites in a total volume of 100  $\mu$ l. Mice also received 100 ng pertussis toxin (List Biological Laboratories Inc, Campbell, CA) i.p. on day of immunization. 7 Days after immunization, draining lymph nodes were collected and single cell suspensions were prepared by gentle disruption between sterile, frosted-glass microscope slides. Cells were washed and resuspended in complete RPMI medium [RPMI + 10% FBS + 1% Pen/strep + 1% Hepes + 1% L-Glutamine] before being seeded in a 96-well tissue culture plate at  $1 \times 10^6$  cells/well. Cells were pre-treated for 30 min with either vehicle (DMSO control) or A-1396076.0 at increasing concentrations and then stimulated with either medium control, PLP antigen (20  $\mu$ g/mL final) or anti-CD3/CD28 Dynabeads (5  $\mu$ l/well, Invitrogen, Carlsbad, CA) for 96 h. Culture supernatants were collected and stored at  $-20^\circ\text{C}$  before IFN $\gamma$  quantification and cell viability was determined using the

CellTiterGlo Assay (Promega, Madison, WI) by following the manufacturer's instructions.

### 2.15. NRF2 dependent gene induction

For in-vivo studies, livers were excised at study termination and total liver weights were recorded. A small section of the liver from each animal was cut and placed into a 1.5 ml Eppendorf tube, flash frozen in liquid nitrogen, and placed on dry ice until final storage at  $-80^\circ\text{C}$ . Liver samples were used to evaluate the induction of NRF2 dependent genes by QuantiGene 2.0 assay (ThermoFisher Scientific, Waltham MA, USA) using a FlexMap3D (Luminex, Austin, TX, USA). Small 10–20 mg frozen liver pieces were homogenized using a FastPrep-24 (MP Biomedical), digested with proteinase k at  $65^\circ\text{C}$  for 30 min, and centrifuged for 10 min at  $15000 \times g$  at room temperature. A mixture of 4  $\mu$ l sample lysate, 36  $\mu$ l homogenizing mixture, and 60  $\mu$ l bead mix was incubated at  $54^\circ\text{C}$ , 600 rpm for 18 h. Technical duplicate wells were prepared for each of 5 replicate animal tissues per treatment group. Standard QuantiGene 2.0 assay protocols were followed for signal amplification and detection for a custom 16 gene panel. Net mean fluorescence intensity (MFI) values for each gene were normalized to the geometric mean of the MFI for the reference genes GAPDH, HPRT1, RPL13A, AND RPL19. Normalized MFI values for each gene were then compared to the values for the samples of the five vehicle-treated animals.

## 3. Results

### 3.1. A-1396076 is a selective NRF2 activator

A-1396076 (Fig. 1) was identified as a NRF2 activator through a combination of KEAP1 binding and cellular assays (Table 1). A-1396076 potently stimulated NRF2 activity in a transfected reporter cell line expressing the antioxidant response element (ARE) luciferase construct with an  $\text{IC}_{50}$  of 0.036  $\mu\text{M}$  that was consistent with its KEAP1 binding affinity of 0.021  $\mu\text{M}$ . Consistent with other NRF2 activators, A-1396076 also inhibited IFN $\gamma$  induced NO production in a concentration-dependent manner in the RAW-267 mouse macrophage cell line, albeit with somewhat higher potency (0.002  $\mu\text{M}$ ). A-1396076 is selective for KEAP1, exhibiting greater than 50-fold selectivity against a broad panel of over 100 receptors, ion channels, and kinases (data not shown). A Cerep (Cell l'Evescault, France) binding screen of 85 G-protein-coupled receptors, enzymes, transporters and ion-channel targets revealed good selectivity for A-1396076 as well as with an in-house bio-profiling functional screen of 20 targets. Additionally, A-1396076 demonstrated no affinity in an in-house kinome profiling screen across 78 kinases.

### 3.2. Efficacy in rat AIA model of arthritis correlates with NRF2 dependent gene induction

To determine whether A-1396076 was efficacious in an arthritis model, we tested it in rat adjuvant induced arthritis. A-1396076 was dosed prophylactically prior to administration of adjuvant and paw

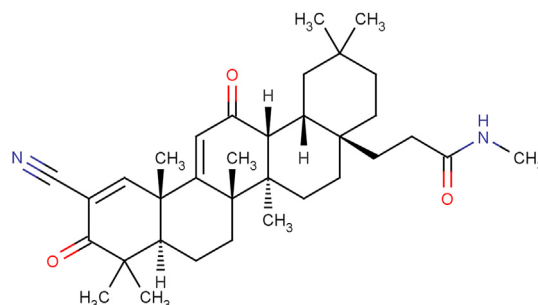


Fig. 1. Structure of A-1396076.

**Table 1**  
In vitro potencies of A-1396076.

Assay	A-1396076.0 EC <sub>50</sub>
ARE reporter	0.036 $\mu$ M SEM 0.0045 $\mu$ M, N = 4
IFN- $\gamma$ induced NO	0.002 $\mu$ M SEM 0.0002 $\mu$ M, N = 22
KEAP1 binding	0.016 $\mu$ M SEM 0.006 $\mu$ M, N = 3

swelling measured over 18 days. As shown in Fig. 2A, A-1396076 dose dependently inhibited paw volume with complete inhibition achieved at the highest dose comparable to the clinical benchmark prednisone. In addition, A-1396076 fully inhibited the bone destruction as assessed by micro-CT analysis of the tarsal bone (Supplemental Figure 1) with similar ED<sub>50</sub>s for both the inflammation and bone endpoints (paw swelling ED<sub>50</sub> = 2.0 mg/kg; bone loss ED<sub>50</sub> = 1.7 mg/kg).

To further assess the relationship between efficacy and target engagement, we measured the liver expression of five Nrf2-regulated genes (SRXN1, GCLC, PTGR, GGT1, and GSTP1) [23,24]. All five genes were induced in the liver in a dose dependent manner (Fig. 2B). GGT1 and GSTP1 demonstrated the most robust induction. Four of the 5 genes demonstrated a similar pattern of induction with comparable ED<sub>50</sub>s (SRXN1 = 1.6 mg/kg; GCLC = 1.7 mg/kg; PTGR = 2.4 mg/kg; GGT1 = 2.0 mg/kg) whereas GSTP1 was approximately 2–3 times more potently activated (ED<sub>50</sub> = 0.6 mg/kg) with near maximal induction at 1 mg/kg. Increases in liver gene expression were associated with the inhibition of

paw swelling (Fig. 2C) suggesting that the anti-inflammatory efficacy of A-1396076 correlates with the pharmacologic modulation of NRF2 activity (Pearson correlation; SRXN1  $r^2 = 0.70$ ,  $p < 0.01$ ; GCLC  $r^2 = 0.89$ ,  $p < 0.001$ ; PTGR  $r^2 = 0.95$ ,  $p < 0.001$ ; GGT1  $r^2 = 0.87$ ,  $p < 0.001$ ; GSTP1  $r^2 = 0.71$ ,  $p < 0.01$ ).

### 3.3. A-1396076 is efficacious in an IFN- $\alpha$ accelerated lupus nephritis model

To further explore the potential of NRF2 activation for treating autoimmune disorders, we tested A-1396076 in a preclinical model of lupus nephritis. Briefly, NZB/W mice are injected with IFN- $\alpha$  expressing adenovirus which induces an accelerated and synchronous disease onset that manifests with anti-double stranded DNA (dsDNA) antibody production and kidney inflammation. Mice treated prophylactically with A-1396076 beginning on day -7, demonstrated a dose dependent delay in onset and severity of proteinuria that led to prolonged survival. (Fig. 3 A/B). The 10 mg/kg dose of A-1396076 inhibited proteinuria and prolonged survival comparable to the clinical comparator mycophenolate mofetil. We did not observe a significant effect on anti-dsDNA antibody titers in this study with either A-1396076 treatment or mycophenolate mofetil (data not shown). To confirm activation of the NRF2 pathway, we evaluated induction of NRF2 dependent gene program by measuring induction of SRXN1 that was used previously and another NRF-2 dependent gene, NQO1 [25]. We observed a dose dependent induction of expression

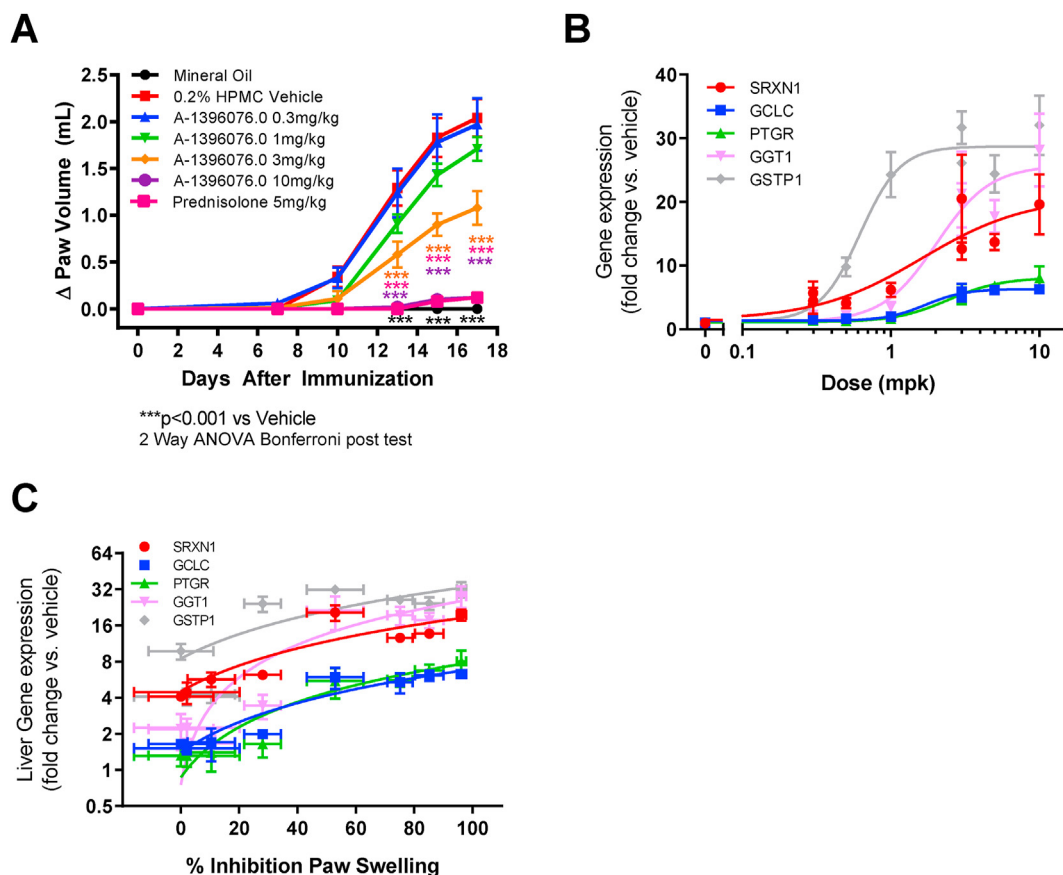


**Fig. 2. A-1396076 inhibition of inflammation in rat AIA correlates with changes in NRF2 dependent gene expression.** Female Lewis rats were given a single intradermal injection of mycobacterium tuberculosis in mineral oil in the right hind paw on day 0. Contralateral paw volumes were measured using a water displacement plethysmometer. Rats were dosed with A-1396076 orally one time per day beginning the day of adjuvant challenge as described in the methods. (A) A-1396076 inhibited swelling as measured by paw volume in rat AIA relative to animals treated with the HPMC vehicle. (n = 9; data is representative of 2 experiments) \*\*\* =  $p < 0.001$  vs. 0.2% HPMC vehicle by two-way ANOVA with Bonferroni post-test. (B). Livers (n = 5 per group) were excised at study termination and were used to evaluate the induction of NRF2 dependent genes using duplicate technical replicates by QuantiGene 2.0 assay. A-1396076 increased NRF2 driven gene expression in the liver of treated animals. (C). Inhibition of paw swelling correlates with the level of NRF2 driven gene expression in the liver (Pearson correlation; SRXN1  $r^2 = 0.70$ ,  $p < 0.01$ ; GCLC  $r^2 = 0.89$ ,  $p < 0.001$ ; PTGR  $r^2 = 0.95$ ,  $p < 0.001$ ; GGT1  $r^2 = 0.87$ ,  $p < 0.001$ ; GSTP1  $r^2 = 0.71$ ,  $p < 0.01$ ). All data is expressed as mean  $\pm$  SEM.

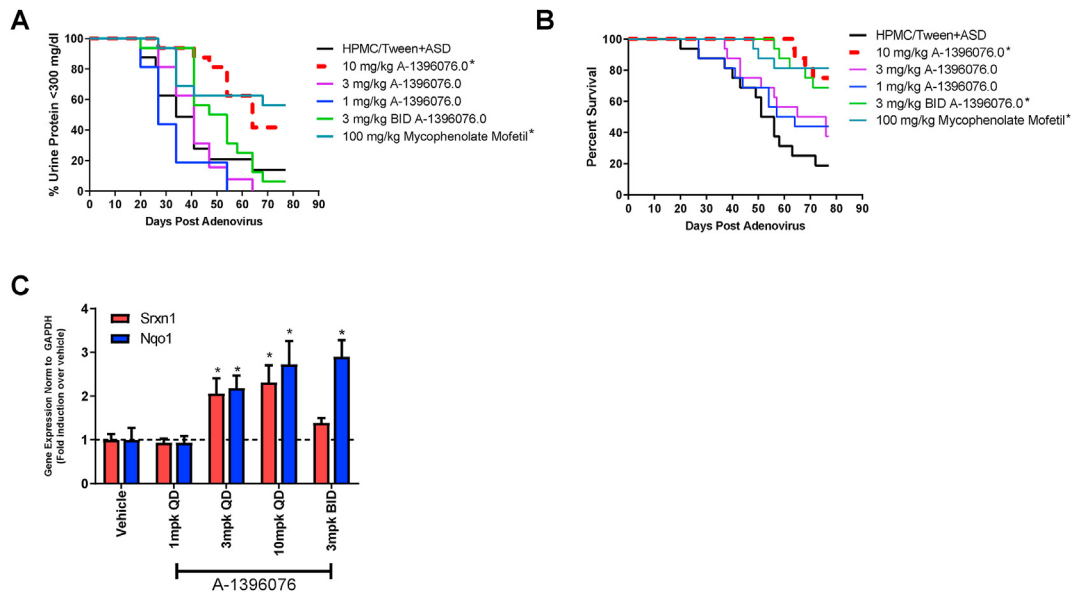


**Fig. 3. A-1396076 decreases proteinuria and improves survival in IFN- $\alpha$  accelerated NZB/W mouse lupus nephritis model.** NZB/W F1 female mice (14 weeks of age) were given an IV injection of  $5 \times 10^9$  IFN $\alpha$ -expressing adenovirus on day 0 and urine protein monitoring was carried out weekly. Mice were dosed orally once per day with A-1396076 or mycophenolate mofetil (100 mg/kg) beginning 7 days prior to administration of IFN- $\alpha$  expressing adenovirus. (A) A-1396076 significantly inhibited the onset of proteinuria ( $>300$  mg/dL) comparable to mycophenolate mofetil ( $n = 16$ ; data is representative of 2 experiments). \* =  $p < 0.05$  vs. vehicle by Mantel-Cox log rank test. (B) A-1396076 significantly prolonged survival comparable to mycophenolate mofetil. \* =  $p < 0.05$  vs. vehicle by Mantel-Cox log rank test. (C) A-1396076 induced nrf-2 dependent gene expression in the liver of treated mice. \* =  $p < 0.05$  vs. vehicle by one-way ANOVA with Dunnett's post-test.

in the liver similar to that observed in the rat AIA model (Fig. 3C).

### 3.4. Efficacy of A-1396076 in multiple inflammatory models requires treatment at time of antigen challenge

A series of experiments to test the efficacy of A-1396076 in antigen induced models of inflammation was undertaken to better understand the role of NRF2 activation in the potential treatment of inflammatory diseases. In a rat collagen induced arthritis (CIA) model, the ability of A-1396076 to inhibit disease in prophylactic and therapeutic modalities was assessed. In this model, rats are first sensitized to collagen on day 0 with antigen boost on day 6 and clinical signs of paw swelling appear on day 11. A-1396076 fully inhibited paw swelling when administered at 10 mg/kg orally once per day starting prior to the boost on day 6; however, no effect was observed when A-1396076 was administered at 10 mg/kg orally once per day starting on day 11 at the first signs on paw swelling (Fig. 4A/B). Prednisolone was dosed at 5 mg/kg orally once per day starting on day 11 and it significantly inhibited paw swelling. In addition to paw swelling, we evaluated anti-collagen antibody titers at the termination of the study. A-1396076 significantly inhibited the levels of anti-collagen antibodies when administered prophylactically but not in the therapeutic modality (supplemental Figure 2).

Similar efficacy was observed in the rat experimental autoimmune encephalomyelitis (EAE) model as well as the mouse GPI-induced model of arthritis. In the EAE model, rats were sensitized to the myelin oligodendrocyte glycoprotein (MOG<sub>1-55</sub>) antigen on day 0 with clinical signs manifesting on day 11. A-1396076 at 10 mg/kg significantly inhibited development of clinical signs when administered at the time of sensitization (prophylactic) but had no effect when administered on day 7 (late-prophylactic) (Fig. 4C/D). The positive control FTY720 significantly inhibited clinical score when dosed at 1 mg/kg starting on day 7. In the GPI model, mice are immunized with GPI (glucose 6 phosphate isomerase) protein on day 0 and develop clinical signs beginning on day 10. A-1396076 dosed once per day at 10 mg/kg ameliorated paw swelling when administered prophylactically but not late-prophylactically (Fig. 4E/F). In both models, we evaluated the expression of NRF2 regulated genes GGT1, SRXN1, GSTP1 in the liver to confirm pharmacologic

activity in both treatment modalities (Supplemental Figure 3). Similar induction of these genes was observed in both treatment groups suggesting that although the NRF2 pathway was engaged in both treatment modes, modulation of this pathway was only efficacious when A-1396076 is administered prior to antigen challenge. The inhibition of paw swelling together with the inhibition of the antibody titers in the rat CIA model suggested that disruption of the antigen dependent lymphocyte activation is a potential operant mechanism for NRF2 activators.

To test this hypothesis, we evaluated the ability of A-1396076 to inhibit inflammation in collagen antibody induced arthritis (CAIA), a passive-transfer model of arthritis that does not require antigen dependent T cell activation. A-1396076 did not significantly inhibit mean arthritis score (MAS) at either dose tested despite inducing NRF2 dependent genes in the liver as observed in the other models (Fig. 5). Taken together, these data support the hypothesis that activation of the NRF2 pathway ameliorates inflammation when treatment occurs at the time of or prior to antigen challenge suggesting that inhibition of lymphocyte priming is a primary mechanism of action for this compound.

### 3.5. NRF2 activation inhibits antigen dependent T cell activation

To determine the cellular mechanism of action we tested the ability of A-1396076 to inhibit antigen specific T cell activation *ex vivo*. Briefly, lymph nodes from mice sensitized to PLP were harvested and then challenged with PLP. A-1396076 dose dependently inhibited this antigen-driven activation as measured by IFN- $\gamma$  production with a clear separation of effect between inhibition of IFN- $\gamma$  production and cell viability (Fig. 6A; IFN- $\gamma = 0.013 \mu\text{M}$ ; viability =  $0.280 \mu\text{M}$ ). Interestingly, when T cells were challenged with anti-CD3/CD28 which bypasses antigen presentation, A-1396076 inhibition of IFN- $\gamma$  was only observed at IC<sub>50</sub> of  $0.35 \mu\text{M}$  which was comparable to the viability IC<sub>50</sub> of  $0.38 \mu\text{M}$  (Fig. 6B). To further confirm these results *in vivo* we evaluated A-1396076 in a mouse model of antigen driven cytokine production. Briefly, mice were immunized with MOG peptide and challenged 5 days later with anti-CD3. The MOG immunization results in a significant increase in IL-17 production compared to unimmunized anti-CD3 challenged mice. We evaluated A-1396076 treatment starting prior to the

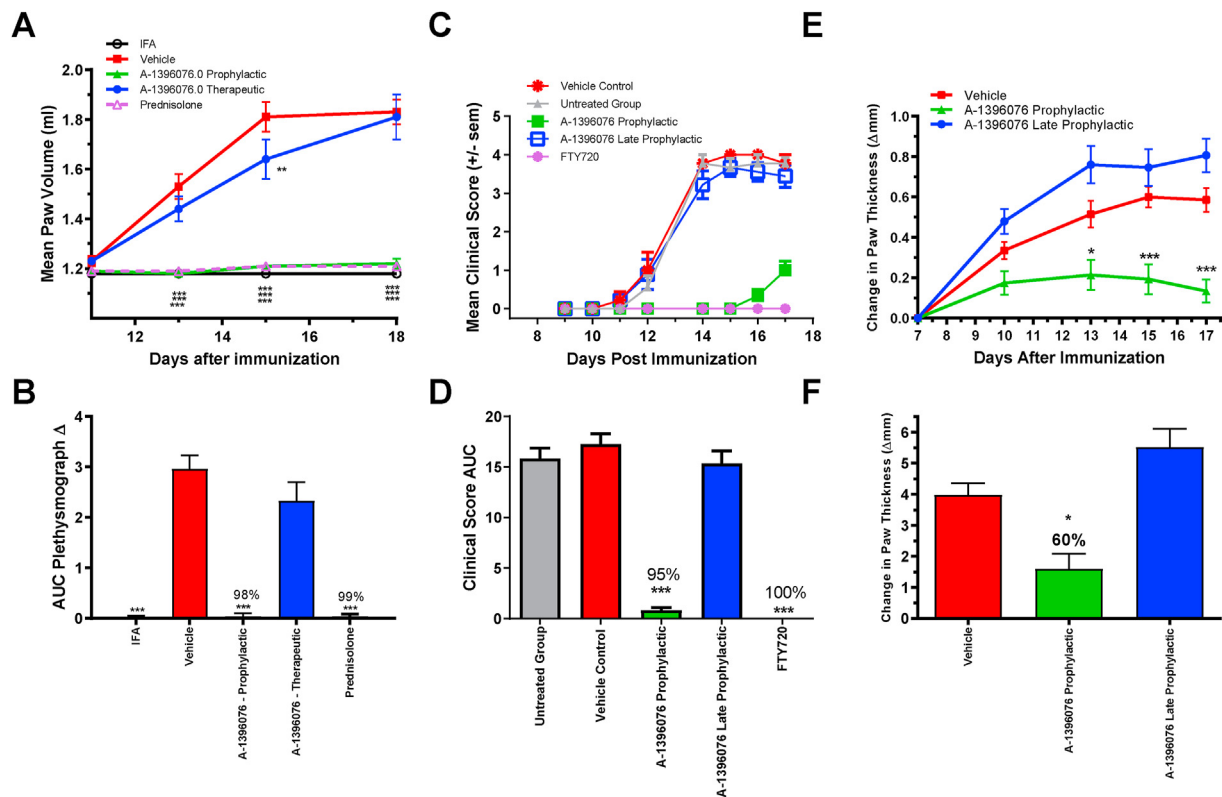


**Fig. 4. A-1396076 inhibits inflammation in autoimmune models only when dosed at the time of antigen challenge.** (A/B) Lewis rats were immunized with bovine type II collagen in IFA intradermally on day 0 and boosted with collagen in IFA on day 6. Paw volume was measured using a micro-controlled volume meter plethysmograph with left and right paw volumes averaged for analysis. Rats were dosed orally BID at 10 mg/kg beginning on day 5 (late prophylactic) or day 11 (therapeutic) with A-1396076. Prednisolone was used as a positive control and was dosed orally QD starting on day 11. After initial collagen immunization on day 0 in the rat CIA model, A-1396076 was administered orally at 10 mg/kg once a day beginning either on day 5 (1 day prior to antigen boost) or day 11 at the onset of clinical signs. Paw swelling was measured by plethysmograph and expressed as mean paw volume by day (A) or AUC from day 8–18 (B) ( $n = 9$ ; one experiment). (C/D) Female Brown Norway rats were immunized with MOG in CFA at the base of the tail. A-1396076 was administered orally once a day at 10 mg/kg beginning either on day 0 prior to immunization (prophylactic) with MOG peptide in CFA or day 7 post immunization prior to the onset of clinical signs (late prophylactic). FTY720 was administered daily (1 mg/kg PO) beginning Day 7. Animals were monitored daily for the onset of clinical signs and scored using the scale: 0 = normal, 1 = limp tail, 2 = abnormal gait, 3 = partial hind limb paralysis, 4 = complete hind limb paralysis, 5 = moribund or dead. Data is expressed as clinical score for each day (C) and expressed as AUC from days 0–17 (D) ( $n = 9$ ; one experiment). (E/F) Male DBA1/J mice were immunized intradermally at the base of the tail with an emulsion containing glucose-6-phosphate isomerase in CFA. A-1396076 was administered orally once a day at 10 mg/kg beginning either on day 0 prior to immunization with GPI (prophylactic) or 7 days post immunization (late prophylactic). Change in paw thickness was assessed by caliper measurements and reported by day (E) and expressed as AUC from days 7–17 (F) ( $n = 15$ ; one experiment). All data is expressed at mean  $\pm$  SEM. \* =  $p < 0.05$ ; \*\* =  $p < 0.01$ ; \*\*\* =  $p < 0.001$  vs vehicle by two-way ANOVA with Bonferroni post-test (A/C/E) or one-way ANOVA with Dunnett's post-test (B/D). All data is expressed at mean  $\pm$  SEM.

MOG immunization or just prior to the anti-CD3 challenge. A-1396076 treatment prior to MOG immunization resulted in significant inhibition of IL-17 production in a dose-dependent manner bringing IL-17 plasma levels down to that of unimmunized anti-CD3 challenged mice (Fig. 6C). In contrast, A-1396076 treatment prior to the anti-CD3 challenge had no significant impact on IL-17 production at any dose tested (Fig. 6D). These data suggest that the mechanism of inhibition T cell cytokine production by NRF2 activation was mediated by antigen presenting cells and not a direct effect on T cells.

It has been reported that DMF, a NRF2 activator, can inhibit MHC Class II expression in dendritic cells [26]. Therefore, we tested whether this occurred *in vivo* utilizing the mouse ovalbumin (OVA)-induced lung inflammation model. In this model, mice are sensitized with OVA and subsequently challenged with either OVA alone or OVA with LPS. While OVA challenge induced lung inflammation and a slight elevation in MHC Class II expression on dendritic cells, mice challenged with OVA + LPS demonstrated a much more robust induction of MHC Class II. Treatment with A-1396076 completely inhibited this induced expression with either OVA or OVA + LPS (Fig. 7A). Similar inhibition was also observed with the costimulatory molecule CD86 (data not shown). In an additional experiment, A-1396076 dose dependently inhibited both MHC Class II

and CD86 with similar ED<sub>50</sub> values as observed in the models of efficacy (Fig. 7B).

#### 4. Discussion

These data describe the pharmacologic properties of A-1396076, a potent and selective small molecule activator of NRF2. A-1396076 binds to KEAP1 with subsequent activation of an ARE-driven gene transcription program as well as inhibition of IFN $\gamma$  induced NO production in the mouse macrophage RAW cell line. We evaluated the efficacy of this molecule in the rat AIA model and demonstrated full efficacy comparable to that achieved by the glucocorticoid prednisone. In addition, there was a significant upregulation of multiple ARE responsive genes downstream of NRF2 including SRXN1, GCLC, PTGR, GGT1 and GGTP1 in the liver. This was associated with a strong correlation between the upregulation of these genes and inhibition of paw swelling in the model. We further evaluated the potential of this mechanism to suppress inflammation in the IFN- $\alpha$  accelerated model of lupus nephritis. A-1396076 significantly inhibited proteinuria and prolonged survival with a concomitant increase in the liver expression of the NRF2 dependent genes SRXN1 and NQO1. These data strongly suggest that NRF2 activation may be the primary

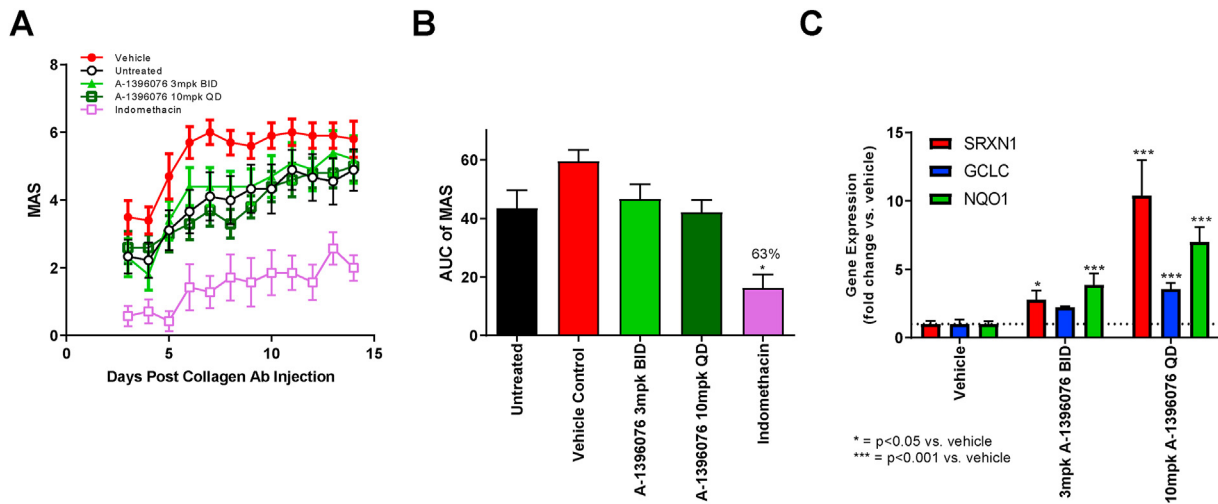


**Fig. 5. Prophylactic A-1396076 treatment does not impact inflammation in CAIA mouse model despite elevation of NRF2 dependent genes.** Female Balb/cN mice were given an intravenous injection of an arthritogenic cocktail of five monoclonal antibodies to type II collagen on day 0, followed on day 3 by an intraperitoneal injection of LPS. Mice were then monitored daily for disease development from day 3 until the conclusion of the experiment. A-1396076 (3 mg/kg BID or 10 mg/kg QD) or indomethacin (1.5 mg/kg QD) were administered orally beginning on day 0 prior to injection of anti-collagen antibody cocktail (prophylactic). Clinical arthritis was assessed in each paw as Mean Arthritic Score (MAS) according to presence of redness and swelling at one or more sites (1), two or more sites (2), or deformity in the paws and stiffness in the joints (ankylosis) (3). Clinical scores were summed across all four paws and are reported either by day (A) or AUC from day 3–14 (B) (n = 12; one experiment). (C) Livers (n = 5 per group) were excised at study termination and were used to evaluate the induction of NRF2 dependent genes using duplicate technical replicates by QuantiGene 2.0 assay. NRF2 dependent gene expression levels were upregulated in the liver of mice that received A-1396076 compared to vehicle controls. \* = p < 0.05; \*\* = p < 0.01; \*\*\* = p < 0.001 vs vehicle by one-way ANOVA with Dunnett’s post-test. All data is expressed at mean ± SEM.

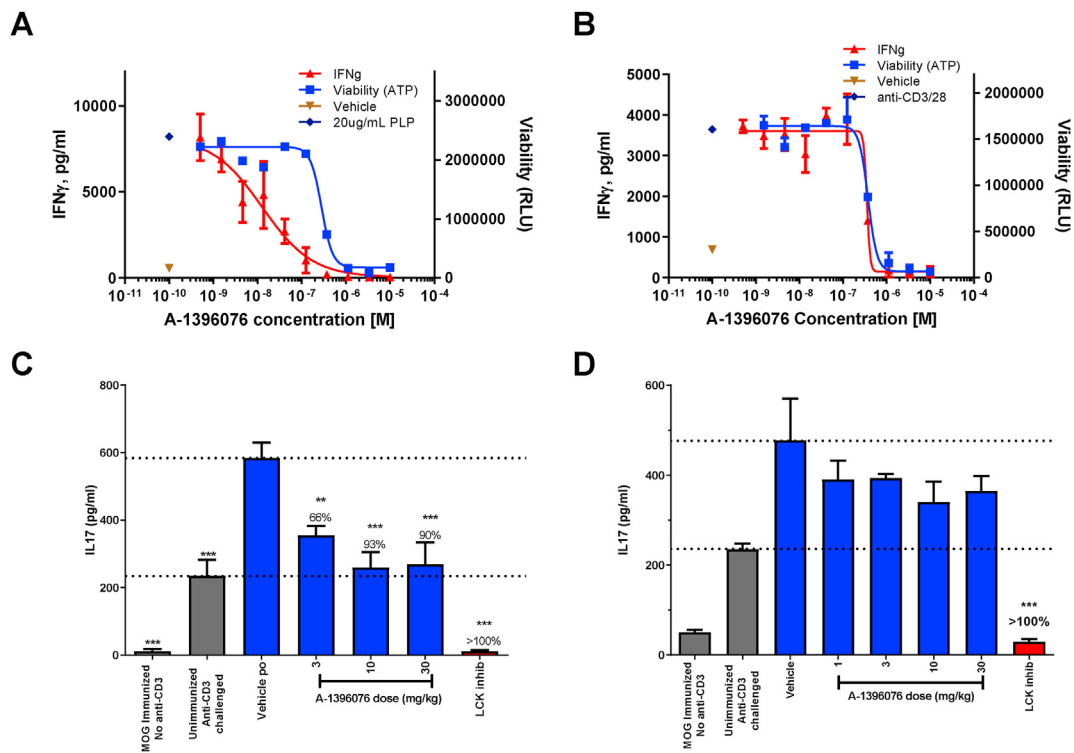


**Fig. 6. A-1396076 inhibits antigen dependent T cell activation.** (A/B) Balb/c mice were immunized subcutaneously with PLP<sub>139-151</sub> in IFA and with pertussis toxin intraperitoneally. 7 days after immunization draining lymph nodes were collected and single cell suspension was prepared. Cells were pre-treated for 30 min with A-1396076 at the indicated concentrations followed by stimulation with PLP (A) or anti-CD3/CD28 (B) for 96 h. IFN $\gamma$  production was measured by ELISA and viability was measured by CellTiterGlo. Technical replicates were performed in duplicate and the data displayed is representative of two individual experiments. (C/D) C57BL/6/N mice were immunized subcutaneously with MOG peptide and *Mycobacterium tuberculosis* H37Ra in IFA on day 0 and challenged intravenously with anti-CD3 antibody on day 5. Mice were bled 2 h following anti-CD3 challenge and IL-17 levels were measured by ELISA. A-1396076 was administered once a day beginning either prior to MOG immunization (C) or immediately prior to anti-CD3 challenge (D). An LCK inhibitor was used as a positive control and was dosed at 30 mg/kg orally 1 h prior to anti-CD3 challenge. (n = 8; one experiment) \*\* = p < 0.01, \*\*\* = p < 0.001 vs vehicle by one-way ANOVA with Dunnett’s post-test. All data is expressed at mean ± SEM.

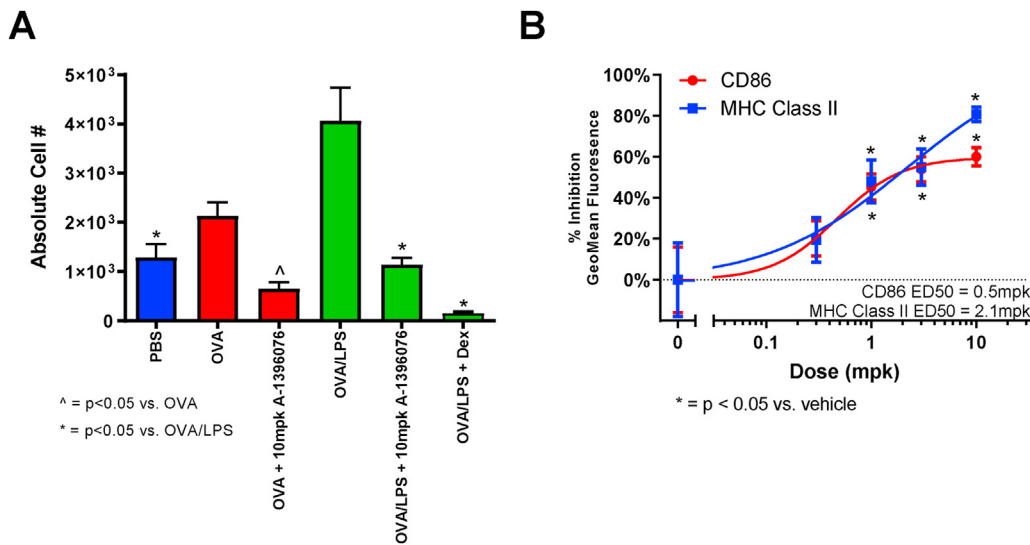


**Fig. 7. A-1396076 inhibits MHC Class II expression induced by intranasal OVA/LPS challenge in mice.** Balb/c mice were sensitized with ovalbumin in alum adjuvant on day 0 and 7 and challenged intranasally with ovalbumin with or without LPS on days 14 and 16. On day 17 bronchoalveolar lavage was performed and cells were analyzed by flow cytometry using anti-CD11c APC, anti-CD80 PCP-Cy5.5, anti-CD86 PE, and anti-MHC Class II FITC antibodies to assess mature dendritic cells (CD11c + MHC Class II hi). Mice were treated orally with 10 mg/kg A-1396076 twice a day beginning on day 13 prior to the intranasal challenge. A) A-1396076 inhibited the number of mature dendritic cells in mice challenged with either OVA alone (red) or OVA plus LPS (green). \* =  $p < 0.05$  vs. OVA and ^ =  $p < 0.05$  vs. OVA/LPS by one-way ANOVA with Dunnett's post-test. B) A-1396076 dose dependently inhibited CD86 and MHC II expression in mice challenged with OVA/LPS ( $n = 10$  per group; one experiment). \* =  $p < 0.05$  vs. OVA/LPS by one-way ANOVA with Dunnett's post-test. All data is expressed at mean  $\pm$  SEM.

mechanism for inhibition of the inflammation by A-1396076 in these studies.

The initiation of an adaptive immune response involves the display of antigen by antigen presenting cells to T cells leading to T cell activation and proliferation with subsequent activation of additional downstream inflammatory pathways. To further explore the temporal component of how NRF2 dependent mechanisms are responsible for this efficacy, we tested A-1396076 in several animal models of disease utilizing both prophylactic and therapeutic settings in order to evaluate the impact of NRF2 activation prior or subsequent to antigen challenge. A-1396076 was efficacious in both the rat CIA and mouse GPI induced arthritis models when administered prophylactically at the time of antigen sensitization but was not effective when administered after antigen challenge. A-1396076 was not efficacious in the therapeutic modality despite demonstrating pharmacologic induction of the NRF2 dependent gene expression program to comparable levels achieved with prophylactic treatment. These data suggest that A-1396076 inhibits inflammation by dampening antigen-dependent immune activation. To test this hypothesis, A-1396076 was administered in the CAIA model which is induced by the passive transfer of anti-collagen antibodies, thus bypassing antigen dependent immune activation. A-1396076 was not efficacious in this model despite induction of the NRF2 dependent genes SRXN1 and NQO1. A similar series of studies in the rat MOG EAE model of multiple sclerosis replicated the pattern of efficacy in the prophylactic but not therapeutic setting suggesting that the anti-inflammatory effect of A-1396076 was dependent on antigen-driven inflammation in models of arthritis and multiple sclerosis.

We evaluated the effects of A-1396076 in an *ex vivo* antigen stimulation assay in order to further refine the cell types and processes that are impacted by A-1396076. Concentration dependent inhibition of PLP induced IFN- $\gamma$  production was achieved with A-1396076 with nearly complete inhibition of cytokine production seen. This effect was specific to antigen-induced activation as A-1396076 did not reduce IFN- $\gamma$  levels independent of the impact on cell viability. We confirmed the antigen-dependence of this mechanism *in vivo* utilizing MOG-sensitization with anti-CD3 challenge. A-1396076 inhibited the MOG-dependent induction of serum IL-17 when dosed at the time of antigen sensitization but had no

effect when administered prior to stimulation with anti-CD3. Together these data support the conclusion that the NRF2 activator A-1396076 suppresses antigen dependent T cell activation.

Inhibition of T cell activation can occur through either direct effect on T cells or an indirect effect by inhibiting the presentation of antigen by professional antigen presenting cells. Several reports have described a link between NRF2 activation and antigen presentation by dendritic cells. Mice with genetically deleted NRF2 have enhanced antigen presentation capacity as reflected by higher levels of MHC Class II, CD86, and CD40 suggesting a role for NRF2 in adaptive immunity [27]. A similar phenotype was induced in human dendritic cells with pharmacologic modulation using DMF, leading to reductions in surface expression of MHC Class II and CD80/86. This caused a decrease in T cell activation as measured by production of IL-17 and IFN- $\gamma$  as well as reduced proliferation [26]. However, it was somewhat surprising that high concentrations of DMF were required to inhibit the DC surface molecules. The data presented here confirm and extend this finding by demonstrating the inhibition of dendritic cell activation markers *in vivo*. Using the mouse OVA-induced lung inflammation model, where surface expression of MHC Class II and CD86 is increased following aerosol OVA challenge, we show that A-1396076 inhibited these DC activation markers when administered prior to challenge. This is the first report to demonstrate a direct effect of a NRF2 activator on this pathway in a whole animal system.

One mechanism by which NRF2 activation could reduce antigen presentation would be the induction of genes related to the inhibition of reactive oxygen species (ROS). ROS play key roles in the activation of dendritic cells and in antigen presentation. Dendritic cells increase ROS levels following stimulation with either LPS or antigen and the antioxidant ebselen inhibits both LPS induced DC activation and antigen dependent T cell activation [28]. Subsequent studies in mouse dendritic cells point to role of ROS in regulating antigen presentation by controlling the pH of phagosomes. In mouse DCs, phagosomes have higher pH values compared to phagosomes from macrophages and this difference is dependent on the activity of NOX2, a NADPH oxidase gene responsible to produce ROS [29,30]. These higher pH values led to an increase in antigen degradation and subsequent reduction in antigen presentation.

Similarly, in human DCs, NOX2 also regulates pH within endosomes and is required for efficient antigen presentation [31]. An additional ROS-dependent mechanism hypothesized to impact antigen presentation is the direct modification of antigens by oxidation that could lead to more efficient proteolytic degradation either by enhancing the activity of proteases or altering the structure of antigens making them more susceptible to proteolysis [29]. In this work, we demonstrate the increased expression of multiple genes involved in the reduction of ROS (SRXN1, GGT, NQO1, TXNRD1) across multiple *in vivo* models of inflammation. The induction of these antioxidant mechanisms may contribute to the reduction in ROS dependent antigen processing and presentation leading to inhibition of T cell activation.

Multiple immune mediated disorders are characterized by epitope spreading of the autoreactive T and B cell response from the initial antigenic epitopes that trigger the immune response to additional endogenous antigens over the course of disease [32]. This has been noted in rheumatoid arthritis (RA), multiple sclerosis (MS), and systemic lupus erythematosus (SLE). In patients with early signs of arthralgia that go on to develop RA, epitope spreading is observed in both anti-citrullinated protein antibodies and rheumatoid factor with early treatment intervention lengthening the time to diagnosis of RA [33]. Epitope spreading was reported in pediatric MS patients who demonstrated reactivity to a broader number of central nervous system antigens when evaluated 3 months after initial disease presentation [34]. In an evaluation of T cell epitopes in SLE, multiple cross-reactive T cell epitopes were identified between the self-antigen SmD, additional lupus auto-antigens, and microbes [35]. This led the study's authors to suggest a role for diverse environmental antigens to contribute to both initial disease onset and flares that occur following remission induced by therapy. We hypothesize that by inhibiting antigen induced T cell activation during the course of chronic inflammatory disease, A-1396076 could reduce epitope spreading that occurs and could be to be an effective therapy to dampen progression of immune mediated diseases if treatment begins early during the development of disease or could prevent worsening of disease as a result of inflammatory flares.

Together these data suggest that activation of NRF2 can dampen the T cell driven inflammatory response to antigens by reducing the activation of T cells by antigen-presenting dendritic cells. Pre-clinical models suggest this may be an effective method for dampening early disease or chronic antigen-driven autoimmune disorders that are propagated by persistent presentation of self-antigens.

#### Author contribution

Christian Goess – Conceptualization, Methodology, Formal analysis, Writing – original draft, Writing – review & editing, Visualization, Sonia Terrillon – Conceptualization, Methodology, Formal analysis, Writing – review & editing, Martha Mayo – Methodology, Formal analysis, Investigation, Writing – review & editing, Peter Bousquet – Conceptualization, Methodology, Formal analysis, Writing – review & editing, Craig Wallace – Methodology, Formal analysis, Investigation, Writing – review & editing, Michelle Hart – Methodology, Formal analysis, Investigation, Writing – review & editing, Suzanne Mathieu – Methodology, Formal analysis, Investigation, Writing – review & editing, Rachel Twomey – Methodology, Formal analysis, Investigation, Writing – review & editing, Diana Donnelly-Roberts – Conceptualization, Methodology, Formal analysis, Investigation, Writing – review & editing, Marian Namovic – Methodology, Formal analysis, Investigation, Writing – review & editing, Paul Jung – Conceptualization, Methodology, Formal analysis, Writing – review & editing, Min Hu – Methodology, Formal analysis, Investigation, Writing – review & editing, Paul Richardson – Methodology, Formal analysis, Investigation, Writing – review & editing, Tim Esbenshade – Conceptualization, Methodology, Writing – review & editing, Carolyn A. Cuff – Conceptualization, Methodology, Writing – original draft, Writing – review & editing

#### Funding disclosure

All authors are employees of AbbVie. The design, study conduct, and financial support for this research were provided by AbbVie. AbbVie participated in the interpretation of data, review, and approval of the publication.

#### Declaration of competing interest

The authors declare the following financial interests/personal relationships which may be considered as potential competing interests:

All authors are employees of AbbVie. The design, study conduct, and financial support for this research were provided by AbbVie. AbbVie participated in the interpretation of data, review, and approval of the publication.

#### Acknowledgements

The authors would like to acknowledge the technical contributions of AbbVie Comparative Medicine East staff for husbandry and dosing of *in vivo* studies.

#### Appendix A. Supplementary data

Supplementary data to this article can be found online at <https://doi.org/10.1016/j.jtauto.2020.100079>.

#### References

- [1] T. Ishii, K. Itoh, S. Takahashi, H. Sato, T. Yanagawa, Y. Katoh, et al., Transcription factor Nrf2 coordinately regulates a group of oxidative stress-inducible genes in macrophages, *J. Biol. Chem.* 275 (2000) 16023–16029.
- [2] K. Itoh, J. Mimura, M. Yamamoto, Discovery of the negative regulator of Nrf2, Keap1: a historical overview, *Antioxidants Redox Signal.* 13 (2010) 1665–1678.
- [3] L.M. Zipper, R.T. Mulcahy, The Keap1 BTB/POZ dimerization function is required to sequester Nrf2 in cytoplasm, *J. Biol. Chem.* 277 (2002) 36544–36552.
- [4] K.I. Tong, Y. Katoh, H. Kusunoki, K. Itoh, T. Tanaka, M. Yamamoto, Keap1 recruits Neh2 through binding to ETGE and DLG motifs: characterization of the two-site molecular recognition model, *Mol. Cell Biol.* 26 (2006) 2887–2900.
- [5] M. McMahon, N. Thomas, K. Itoh, M. Yamamoto, J.D. Hayes, Dimerization of substrate adaptors can facilitate cullin-mediated ubiquitylation of proteins by a "tethering" mechanism: a two-site interaction model for the Nrf2-Keap1 complex, *J. Biol. Chem.* 281 (2006) 24756–24768.
- [6] S.-C. Lo, X. Li, M.T. Henzl, L.J. Beamer, M. Hannink, Structure of the Keap1:Nrf2 interface provides mechanistic insight into Nrf2 signaling, *EMBO J.* 25 (2006) 3605–3617.
- [7] K. Yoh, K. Itoh, A. Enomoto, A. Hirayama, N. Yamaguchi, M. Kobayashi, et al., Nrf2-deficient female mice develop lupus-like autoimmune nephritis, *Kidney Int.* 60 (2001) 1343–1353.
- [8] N. Maicas, M.L. Ferrandiz, R. Brines, L. Ibanez, A. Cuadrado, M.I. Koenders, et al., Deficiency of Nrf2 accelerates the effector phase of arthritis and aggravates joint disease, *Antioxidants Redox Signal.* 15 (2011) 889–901.
- [9] C.J. Wruck, A. Fragoulis, A. Gurzynski, L.O. Brandenburg, Y.W. Kan, K. Chan, et al., Role of oxidative stress in rheumatoid arthritis: insights from the Nrf2-knockout mice, *Ann. Rheum. Dis.* 70 (2011) 844–850.
- [10] C.M. Larabee, S. Desai, A. Agasing, C. Georgescu, J.D. Wren, R.C. Axtell, et al., Loss of Nrf2 exacerbates the visual deficits and optic neuritis elicited by experimental autoimmune encephalomyelitis, *Mol. Vis.* 22 (2016) 1503–1513.
- [11] C.Y. Fu, J. Chen, X.Y. Lu, M.Z. Zheng, L.L. Wang, Y.L. Shen, et al., Dimethyl fumarate attenuates lipopolysaccharide-induced mitochondrial injury by activating Nrf2 pathway in cardiomyocytes, *Life Sci.* 235 (2019) 116863.
- [12] Y. Yamaguchi, H. Kanzaki, Y. Katsumata, K. Itohiya, S. Fukaya, Y. Miyamoto, et al., Dimethyl fumarate inhibits osteoclasts via attenuation of reactive oxygen species signalling by augmented antioxidant, *J. Cell Mol. Med.* 22 (2018) 1138–1147.
- [13] J. Bruck, R. Dringen, A. Amasuno, I. Pau-Charles, K. Ghoreschi, A review of the mechanisms of action of dimethylfumarate in the treatment of psoriasis, *Exp. Dermatol.* 27 (2018) 611–624.
- [14] X. Liu, W. Zhou, X. Zhang, P. Lu, Q. Du, L. Tao, et al., Dimethyl fumarate ameliorates dextran sulfate sodium-induced murine experimental colitis by activating Nrf2 and suppressing NLRP3 inflammasome activation, *Biochem. Pharmacol.* 112 (2016) 37–49.
- [15] J. Han, S. Ma, H. Gong, S. Liu, L. Lei, B. Hu, et al., Inhibition of acute graft-versus-host disease with retention of graft-versus-tumor effects by dimethyl fumarate, *Front. Immunol.* 8 (2017) 1605.
- [16] S. Schilling, S. Goelz, R. Linker, F. Luehder, R. Gold, Fumaric acid esters are effective in chronic experimental autoimmune encephalomyelitis and suppress macrophage infiltration, *Clin. Exp. Immunol.* 145 (2006) 101–107.

- [17] U. Schulze-Topphoff, M. Varrin-Doyer, K. Pekarek, C.M. Spencer, A. Shetty, S.A. Sagan, et al., Dimethyl fumarate treatment induces adaptive and innate immune modulation independent of Nrf2, *Proc. Natl. Acad. Sci. U. S. A* 113 (2016) 4777–4782.
- [18] G.O. Gillard, B. Collette, J. Anderson, J. Chao, R.H. Scannevin, D.J. Huss, et al., DMF, but not other fumarates, inhibits NF-kappaB activity in vitro in an Nrf2-independent manner, *J. Neuroimmunol.* 283 (2015) 74–85.
- [19] M.D. Kornberg, P. Bhargava, P.M. Kim, V. Putluri, A.M. Snowman, N. Putluri, et al., Dimethyl fumarate targets GAPDH and aerobic glycolysis to modulate immunity 360, *Science*, New York, NY, 2018, pp. 449–453.
- [20] R.K. Thimmulappa, R.J. Fuchs, D. Malhotra, C. Scollick, K. Traore, J.H. Bream, et al., Preclinical evaluation of targeting the Nrf2 pathway by triterpenoids (CDDO-Im and CDDO-Me) for protection from LPS-induced inflammatory response and reactive oxygen species in human peripheral blood mononuclear cells and neutrophils, *Antioxidants Redox Signal.* 9 (2007) 1963–1970.
- [21] B.L. Probst, I. Trevino, L. McCauley, R. Bumeister, I. Dulubova, W.C. Wigley, et al., RTA 408, A novel synthetic triterpenoid with broad anticancer and anti-inflammatory activity, *PLoS One* 10 (2015), e0122942.
- [22] D.W. Borhani, D.J. Calderwood, M.M. Friedman, G.C. Hirst, B. Li, A.K. Leung, et al., A-420983: a potent, orally active inhibitor of I $\kappa$ B with efficacy in a model of transplant rejection, *Bioorg. Med. Chem. Lett* 14 (2004) 2613–2616.
- [23] F.X. Soriano, P. Baxter, L.M. Murray, M.B. Sporn, T.H. Gillingswater, G.E. Hardingham, Transcriptional regulation of the AP-1 and Nrf2 target gene sulfiredoxin, *Mol. Cell.* 27 (2009) 279–282.
- [24] J.-M. Lee, M.J. Calkins, K. Chan, Y.W. Kan, J.A. Johnson, Identification of the NF-E2-related factor-2-dependent genes conferring protection against oxidative stress in primary cortical astrocytes using oligonucleotide microarray analysis, *J. Biol. Chem.* 278 (2003) 12029–12038.
- [25] A.T. Dinkova-Kostova, P. Talalay, NAD(P)H:quinone acceptor oxidoreductase 1 (NQO1), a multifunctional antioxidant enzyme and exceptionally versatile cytoprotector, *Arch. Biochem. Biophys.* 501 (2010) 116–123.
- [26] H. Peng, M. Guerau-de-Arellano, V.B. Mehta, Y. Yang, D.J. Huss, T.L. Papenfuss, et al., Dimethyl fumarate inhibits dendritic cell maturation via nuclear factor kappaB (NF-kappaB) and extracellular signal-regulated kinase 1 and 2 (ERK1/2) and mitogen stress-activated kinase 1 (MSK1) signaling, *J. Biol. Chem.* 287 (2012) 28017–28026.
- [27] H.X. Aw Yeang, J.M. Hamdam, L.M. Al-Huseini, S. Sethu, L. Djouhri, J. Walsh, et al., Loss of transcription factor nuclear factor-erythroid 2 (NF-E2) p45-related factor-2 (Nrf2) leads to dysregulation of immune functions, redox homeostasis, and intracellular signaling in dendritic cells, *J. Biol. Chem.* 287 (2012) 10556–10564.
- [28] H. Matsue, D. Edelbaum, D. Shalhevet, N. Mizumoto, C. Yang, M.E. Mummert, et al., Generation and function of reactive oxygen species in dendritic cells during antigen presentation, *J. Immunol.* 171 (2003) 3010–3018.
- [29] F. Kotsias, E. Hoffmann, S. Amigorena, A. Savina, Reactive oxygen species production in the phagosome: impact on antigen presentation in dendritic cells, *Antioxidants Redox Signal.* 18 (2013) 714–729.
- [30] A. Savina, C. Jancic, S. Hugues, P. Guermonprez, P. Vargas, I.C. Moura, et al., NOX2 controls phagosomal pH to regulate antigen processing during crosspresentation by dendritic cells, *Cell* 126 (2006) 205–218.
- [31] A.R. Mantegazza, A. Savina, M. Vermeulen, L. Pérez, J. Geffner, O. Hermine, et al., NADPH oxidase controls phagosomal pH and antigen cross-presentation in human dendritic cells, *Blood* 112 (2008) 4712–4722.
- [32] C.L. Vanderlugt, S.D. Miller, Epitope spreading in immune-mediated diseases: implications for immunotherapy, *Nat. Rev. Immunol.* 2 (2002) 85–95.
- [33] W.J.J. Falkenburg, D. van Schaardenburg, Evolution of autoantibody responses in individuals at risk of rheumatoid arthritis, *Best Pract. Res. Clin. Rheumatol.* 31 (2017) 42–52.
- [34] F.J. Quintana, B. Patel, A. Yeste, M. Nyirenda, J. Kenison, R. Rahbari, et al., Epitope spreading as an early pathogenic event in pediatric multiple sclerosis, *Neurology* 83 (2014) 2219–2226.
- [35] Z. Zhao, J. Ren, C. Dai, C.C. Kannapell, H. Wang, F. Gaskin, et al., Nature of T cell epitopes in lupus antigens and HLA-DR determines autoantibody initiation and diversification, *Ann. Rheum. Dis.* 78 (2019) 380–390.